SLAC-PUB-9519
September 2002

Participants who Contributed Talks to the T1 Group

David Asner (LLNL), Ralph Assmann (CERN), Giovanni Bonvicini (Wayne State U.), Reinhard Brinkmann (DESY), Philip Burrows (Oxford U.), Javier Cardona (BNL), Dmitri Denisov (FNAL), James Early (LLNL), Josef Frisch (SLAC), Jeffrey Gronberg (LLNL), Ramesh Gupta (BNL), Linda Hendrickson (SLAC), Stan Hertzbach (U. of Massachusetts), Tony Hill (LLNL), John Johnstone (FNAL), Bruce King (BNL), Eberhard Keil (CERN), Mieczyslaw Krasny (LPNHE Paris), Michael Lamm (FNAL), Thomas Markiewicz (SLAC), John Marriner (FNAL), Thomas Mattison (UBC), Michiko Minty (DESY), Nikolai Mokhov (FNAL), Katsunobe Oide (KEK), Brett Parker (BNL), Stephan Peggs (BNL), Fulvia Pilat (BNL), Pantaleo Raimondi (SLAC), Peter Schuler (DESY), Daniel Schulte (CERN), John Seeman (SLAC), Mike Seidel (DESY), Tanaji Sen (FNAL), Andrei Seryi (SLAC), Ronald Settles (MPI), Ken Skulina (LLNL), Steve Smith (SLAC), Michael Sullivan (SLAC), Michael Syphers (FNAL), Toshiaki Tauchi (KEK), Valery Telnov (Budker INP/DESY), Peter Tenenbaum (SLAC), Kathleen Thompson (SLAC), Karl van Bibber (LLNL), Mayda Velasco (Northwestern U.), Nicholas Walker (DESY), Peter Wanderer (BNL), Ferdinand Willeke (DESY), Michael Woods (SLAC)

Summary Report of the Interaction Region Working Group at Snowmass 2001

T.W. Markiewicz*
Stanford Linear Accelerator Center
F. Pilat†
Brookhaven National Laboratory

(Dated: January 23, 2002)

The Interaction Region Working Group (T1) at Snowmass 2001 reviewed the issues, designs, and plans of existing and proposed colliders, including hadron colliders, e^-hadron colliders, e^+e^- and $\gamma\gamma$ linear colliders, e^+e^- circular colliders, and muon colliders. This document summarizes the IR issues, status, and R&D plans for each project.

I. INTRODUCTION

The Interaction Region Working Group (T1) reviewed the issues, designs, and plans of existing and proposed colliders, including hadron colliders, e^-hadron colliders, e^+e^- and $\gamma\gamma$ linear colliders, e^+e^- circular colliders, and muon colliders. This document summarizes the IR issues, status, and R&D plans for each project.

II. HADRON COLLIDERS

A. Introduction

The Interaction Region Working group reviewed the Interaction Region systems of existing hadron colliders, such as the Tevatron and RHIC, and of the LHC, now in the construction phase, with the goal of identifying the principal issues to be addressed in the design and planning of a new generation of hadron colliders. In order to have consistent sets of parameters from which to draw concrete examples, the new generation of hadron colliders in this report consists of the Stage 1 and Stage 2 VLHC, as proposed in the VLHC Design Report. [1] The operational experience of existing machines has been taken into consideration as well, since commissioning and operational aspect of the interaction regions must be integrated in the design from the start, as well as the requirements from the experiments.

Table I below summarizes the main characteristics of existing and planned hadron colliders in the world.

The main issues for the planning of future hadron colliders are the overall design and layout, the performance limitations, the development of accelerator IR systems, primarily the final focus IR magnets and powering devices, correction and feedback systems, energy deposition in the IR components and background in the

*twmark@SLAC.Stanford.edu
†pilat@BNL.gov
Stanford Linear Accelerator Center, Stanford University, Stanford, CA 94309, USA
*Work supported in part by Department of Energy Contract DE-AC03-76SF00515.

TABLE I: Main characteristics of existing and planned hadron colliders.

machine	species	rings	magnets	Energy/beam	Luminosity	# of IR's
Tevatron	P pbar	1	1 in 1	1 TeV	8.6 10^{31} (run II-A) 1.4 10^{32}(run II-B)	2
RHIC	Au-Au p-p (p-A)	2	1 in 1	100 GeV/n 250 GeV	2 10^{26}2 10^{32}	6 (4)
LHC	p-p Pb-Pb	2	2 in 1	7 TeV 2.76 TeV/n	2 10^{34} 10^{27}	8 (4)
SSC	p-p	2	1 in 1	20 TeV	10^{33}	2
VLHC-1	p-p	2	2 in 1 (TLM)	20 TeV	1 10^{34}	2
VLHC-2	p-p	2	2 in 1	87.5 TeV	2.7 10^{34}	2

experiments, and finally the integration, from the start, of machine and experiments components. This report will discuss these points in more details in the following sections, together with the main R&D activities that should be undertaken towards the goal of resolving the IR technical challenges.

B. IR design

The Tevatron, RHIC and the LHC IR design rely on anti-symmetric triplet optics to focus the beam at the interaction point (IP). In the Tevatron the protons and antiprotons share the same beam pipe and the orbit are separated by electrostatic separators, allowing them to collide only at D0 and B0, thus minimizing parasitic collisions at the other IP's. The beta squeeze is done at collision energy, with minimal beam loss, over about 100 seconds, and during the beta squeeze the tune shifts are less than 0.03 for antiprotons and 0.01 for protons. RHIC also has an anti-symmetric triplet optics, with the beam horizontally separated before the triplets by the DX and D0 IR dipoles. A beta squeeze from the injection value of 10m to 5m is done during the ramp with plans to squeeze to the design 2m (or further to 1m) at collision energy. In the LHC the triplets are common to the two beams while the beam is separated into the 2 rings downstream by the IR dipoles, warm in the experimental IP1 and IP5 IRs and super-conducting in the other IRs.

An anti-symmetric triplet optics similar to existing colliders is the natural choice for a 20 TeV Stage 1 VLHC IR. (see Figure 1). Triplets of 300 T/m and 4 IR matching quadrupoles of 70 T/m provide the necessary matching flexibility to keep a constant phase advance through the interaction region and allow the beta at the IP to vary between 6 m at injection and 0.3 m in collision optics. A crossing angle of 77 μrad insures 10 σ separation at the first parasitic bunch crossing. The main challenge of this IR design is to develop final focus quadrupole gradients of $\sim$300 T/m and this will be addressed in the IR magnet section below.

The 87.5 TeV Stage 2 VLHC, the first hadron collider to operate in a synchrotron light regime, opens the possibility of flat beams. Emittance and β^* ratios respectively of 0.1 are possible. The main advantage of a flat beam is the minimization of the long-range parasitic crossings and consequently of the long-range beam-beam tune shift, the main IR performance limitation. Both a triplet solution (round beams) and a doublet solution (flat beams) are possible for the Stage-2 VLHC.

The triplet solution for Stage-2 is similar to Stage 1 (Figure 1) but the final focus triplet gradients rise to 400 T/m and likewise the 4 matching quadrupoles also require 400 T/m gradients. In the round optics the final triplet focuses both beams, allowing for a simpler single aperture design. The IR phase advance can be kept constant and the IR is tunable from β^* of 12 m at injection to 0.5 m at collision. A crossing angle of 28.8 μrad insures a 10 σ separation at the first parasitic bunch crossing.

A flat beam, symmetric doublet optics, is very similar to e+e- ring colliders, and with a doublet of respectively 600 and 400 T/m provides likewise fixed phase advance and a β^* tunability from 7.12 m to 0.37 m vertically and from 71.2 m to 3.7 m horizontally. The symmetric doublet optics however requires beam separation immediately after the IP and thus a very challenging 2-in-1 magnet design for the final doublet, with gradients in the 400-600 T/m range. Design options and challenges for the doublet IR magnets will be discussed in the section about IR magnets below.

The main advantage of flat beams is the lower long-range beam-beam tune shift. Table II below compares the performance of round beams and flat beams, all other relevant parameters being equal.

Other than the already mentioned more difficult design of the final focus doublet another potential disadvantage of a flat optics is the lower energy tunability since the flat beam lose their advantage at lower energies where synchrotron radiation is no longer significant.

The main progress at the workshop has been the realization that a 4-magnet final focus solution is possible [2], that can provide both flat and round optics with a continuous transition from doublet to triplet optics,

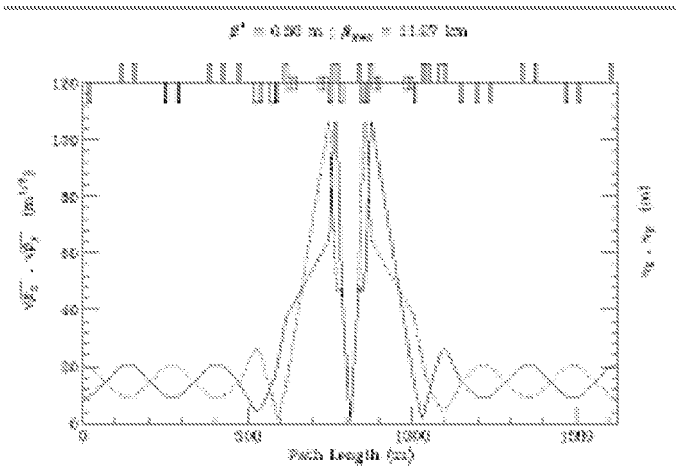

FIG. 1: IR design for the VLHC-Stage 1, collision configuration, with round beam and anti-symmetric triplet optics.

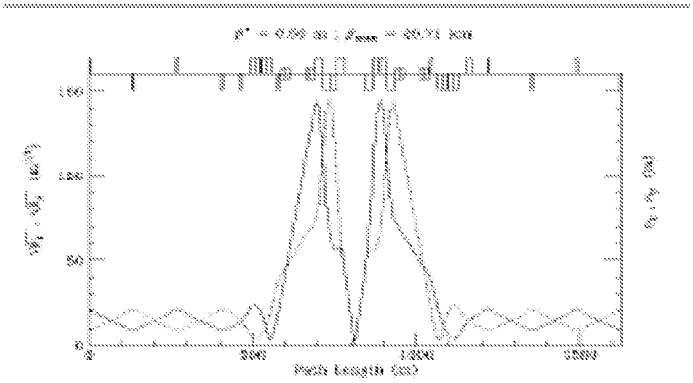

FIG. 2: IR design for VLHC-Stage 2, collision configuration, with round beams and anti-symmetric triplet optics.

an operationally very attractive option, since it has the potential of retaining the advantages of both optics solutions in different energy regimes.

More work is needed to finalize the optics design and to design realistic magnets but having the flexibility of both option is clearly an advantage from the operational point of view by allowing a staged commissioning of flat beams and by retaining the possibility of round beams at lower energies and flat beam at the higher energies to take fully advantage of synchrotron radiation. R&D in IR design will focus on developing an optimal solution that provides both flat and round beam options. About 2 FTE's are required for the design; the R&D issues for the IR magnets will be addressed in section II C below.

TABLE II: Comparison of the long-range beam-beam tune shift for the flat and round beam options for VLHC Stage 2.

	Flat beams	Round beams
Flatness parameter	0.1	1
Beam-beam parameter	0.008	0.008
Peak luminosity (10^{34})	2	2
Total crossing angle (μrad)	10	10
Separation distance	30	120
N of long range collisions / IR	20	84
Long range tune shift /IR -horizontal	0.0008	0.0166
Long range tune shift/IR -vertical	0.0081	0.0166

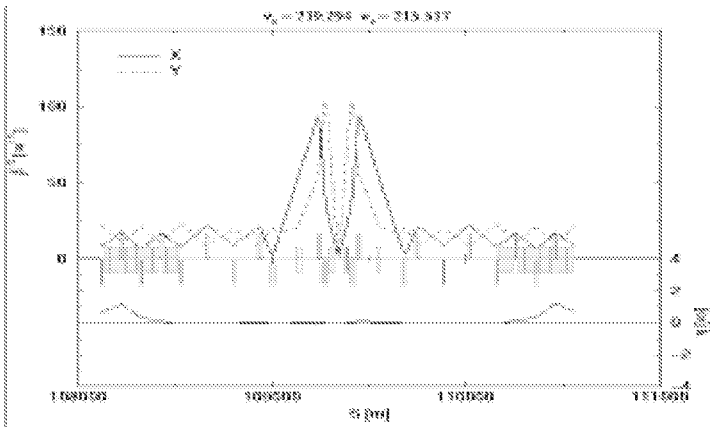

FIG. 3: IR design for VLHC-Stage 2, collision configuration, with flat beams and symmetric doublet optics.

C. IR performance limitations

The main performance limitations of hadron collider IRs are the long-range beam-beam tune shift, field quality in the final focus IR magnets, alignment and mechanical stability in the IR magnets. Traditionally, the performance of hadron accelerators at collision have been analyzed in terms of dynamic aperture, the main figure of merit of long term simulations, modeling the effects of beam-beam interactions, field and alignment errors. However, with the VLHC where the transverse beam dimensions are negligible with respect to the beam pipe and the good field region, (beams sizes are a fraction of a millimeter even at the maximum beta positions in the final focus quadrupoles), a more appropriate figure of merit for the new dynamics regime may be an "operational aperture" where closed orbit control in the IRs plays a more fundamental role than functional dependence on transverse amplitude.

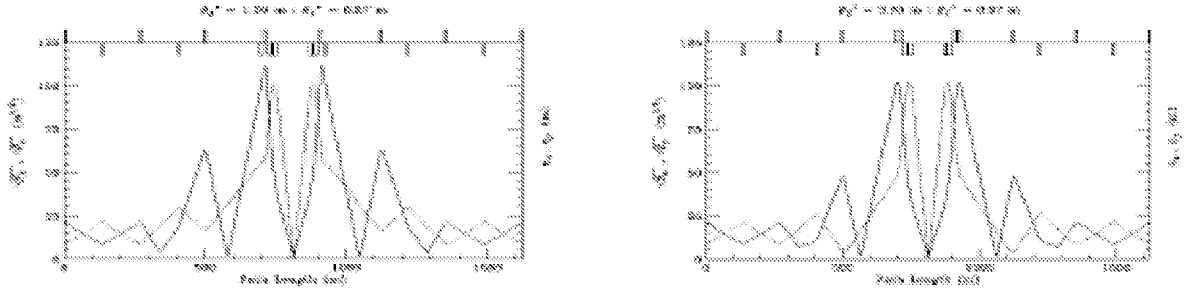

FIG. 4: The left figure shows the flat optics for Stage 2 VLHC (doublet); the figure on the right shows the round optics for Stage 2 VLHC (triplet).

1 Long range beam-beam effects

Long-range beam-beam effects are expected to be the main performance limitation at the Tevatron and at the LHC. Simulation results for the Tevatron (Run II-a, with 36x36 bunches in 3 trains of 12 bunches each) are summarized in Table III below.

Long-range beam-beam effects are the main effect of the dynamic aperture, and the dynamic aperture depends on the bunch number (differences between the head and tail bunch in the train are $\sim 2\sigma$ after 10^6 turns). A crossing angle is henceforth necessary to ensure machine performance. Similar results are obtained for the LHC, where the long range beam-beam effects is predicted to be the limiting effects not only at collision but also at injection energy.

2 Field quality in the IR magnets

This is driven by the crossing angle and luminosity requirements at the IP. A figure of merit for field harmonics at the upper end of injection and beta squeeze is one unit of un-allowed harmonics. To achieve field quality control of this level, experience in the production of RHIC and LHC IR magnets established that a process of optimization between magnet design and correction systems is necessary, determined by the accelerator physics and magnet construction requirements. Figure 5 describes the process that leads to the ultimate field quality as a compromise between magnet production and operational functionality. Further discussion about IR correction schemes will follow in Section II E.

3 Alignment and mechanical stability

Magnet alignment contributes in three major ways to the proper operation of the accelerator. First, misalignment leads to luminosity loss, by steering the beams to the wrong location in the IP. Second, misalignment causes the beam to populate off- axis areas of the aperture and thus become susceptible to harmonic errors that grow in powers of the radius. This is particularly critical for beams with crossing angles. This leads to a decrease in dynamic aperture if not properly accounted for with local correction. Finally, transverse misalignment can lead to a reduction in physical aperture, as beam pipe apertures are possibly already reduced by absorber materials. An analysis of the IR alignment requirements have been carried out for the LHC, where alignment requirements have been tabulated in a Reference Alignment Table (see Figure 6 below) that is useful to analyze alignment requirements for the VLHC. The table relates the accelerator physics requirements to the achievable mechanical tolerances and the accuracy of realistic measurements.

D. IR magnets and power systems

The development of a new generation of IR magnets is critical for future hadron colliders. These require at the same time high gradients, large apertures to accommodate absorbers and crossing angles, excellent field quality to not limit the dynamic aperture, stringent alignment and mechanical stability, all that in a high radiation environment that causes high heat deposition. Attention must also be paid to quench protection and magnet powering schemes. The design of main ring magnets is driven by cost driven by cost since they are typically industrially produced. The design of IR magnets, fewer in number and typically more challenging, is driven by performance.

As these magnets form the final focus, they are located as close as practically possible to the interaction point and they need high gradients to achieve the required β^* with a limited focusing lever arm. The large aperture is required to accommodate absorbers in the beam pipe to intercept the large radiation and heat deposition due to interaction debris. It is also needed to account for lattice requirements for large dynamic aperture and for beam separation from a beam-crossing angle.

The protection goals for IR magnets are comparable to other super-conducting magnets: namely limiting the peak voltage to ground to 1000 V and limiting the peak temperatures to 400 K. These goals are challenging because of the high field and large aperture, which translates into high currents and/or large inductances and large stored energies. Inner triplet magnets are typically powered in series, with the possibility of varying the field in one of the triplet quadrupoles for accelerator studies. In the case of RHIC and LHC the powering scheme has additional complications. The RHIC IR magnets are powered in series with the arc dipole bus and require several layers of nested small current supplies. The LHC inner triplet consists of magnets made from two designs with very different currents.

TABLE III: Predicted performance of the Tevatron with 36x36 bunches.

Error sources	*Average DA (100 K turns)*	*Minimum DA (100 K turns)*
IR magnet errors	18.7	17.0
Head-on beam-beam + IR errors	15.5	13.6
All beam-beam	12.9	8.1
All beam-beam + IR errors	11.3	8.6

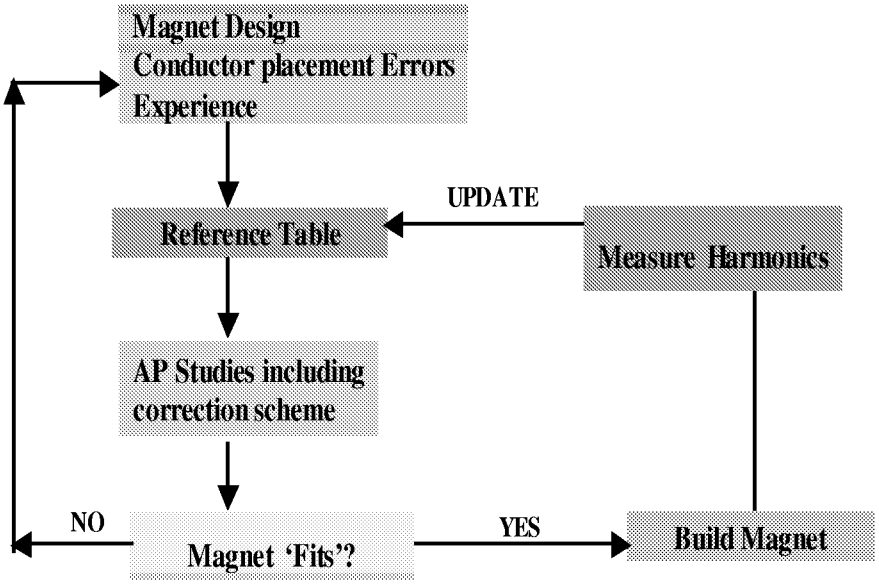

FIG. 5: Process of optimization of field quality for IR magnets.

The state of the art interaction region quadrupoles for the Tevatron, RHIC, and LHC are made from Rutherford style NbTi cables. The 70 mm aperture LHC inner triplet quadrupoles operate in super-fluid with a peak operating gradient of 215 T/m. Future accelerator applications will require a combination of higher gradient, possibly larger aperture and higher heat loads. This means building magnets with Nb_3Sn or HTS (High Temperature Superconductors) materials. The upgrade for the LHC IRs is an excellent opportunity to use NB_3Sn technology for a production series of accelerator magnets. The experience from all phases of the magnet production, from cable procurement through construction and test will be invaluable for the VLHC program.

IR magnets R&D can be organized along 2 paths:

- near term: LHC upgrade and VLHC-1 single aperture Nb_3Sn
- longer term (VLHC-2 double aperture HTS or Nb_3Sn

An R&D program for VLHC Stage 1 magnets can be based on the program planned for the large single bore high gradient quadrupoles for the LHC upgrade. The 2^{nd} generation LHC IR quadrupoles have the following parameters: 90m bore, maximum gradient of 250 T/m and they are based on available Nb_3Sn strands. The main R&D issues are design, fabrication technology, field quality, quench performance, cooling, and quench protection. A possible schedule has a short model built by FY02-FY05 for ~9M$, a prototype around FY05-FY08 for ~18M$, and a production magnets by FY08-FY12 for ~39M$.

The LHC upgrade program would be very important for as a test bench for R&D and production for VLHC-1, since it would be the first large scale application of Nb_3Sn in accelerator magnets, which requires procurement of relatively large volume of Nb_3Sn strand.

Possible parameters for VLHC-1 IR magnets are: 70 mm bore, maximum gradient of 300 T/m , and would require R&D Nb_3Sn strands with critical current larger than 3 kA/mm^2. R&D issues are very similar to the LHC IR upgrade magnets and the R&D plan could call for a short model by FY05-FY08 for ~10M$ and a prototype by FY08-FY10 for ~20M$, with a production magnet time schedule depending on the prototype performance.

R&D of IR magnets for VLHC-2 will focus on magnet development with A15 or HTS or other materials and their radiation hardness, since they will have to withstand high level of radiation. Magnet design will focus on:

Single bore high gradient quadrupoles for round beam optics, with 50-60mm bore and gradients of ~400T/m. An R&D schedule could have a short model by FY12-FY16 for ~12M$.

Double bore high gradient quadrupoles for flat beam optics, with gradients up to 600T/m. A lot of effort

	AP Requirements	Mechanical Tolerances	Measurement and Survey Accuracy	
1a) Single MQX cold mass	Not limiting as long as <=0. Needs further study		Mechanical meas. Not limiting	
Straightness H and V		< 0.1 mm/meter		
Twist		< 0.1 mrad/meter		
1b) Single cold/warm connection MQ	Moved to 2b			
2a) Relative alignment of MQX magnets in composite Q2		Mechanical tests scheduled starting in 2000	Mech. and stretch wire with survey equip.	
Q2a/Q2b transverse alignment	300-500 µm			100 µm
Q2a/Q2b relative roll	1 mrad (rms)			100 µrad (rms)
Q2a/Q2b relative pitch and yaw	100 µrad			130 µrad
2b) Relative alignment of corrector in a composite Q2 and Q3			Should be able to do with mech measurements	
Corrector displacement	500 µm			
Corrector roll	5 mrad			
3) Placement of composite cold mass into cryostat and relating magnetic axis to external fiducial			Only includes errors relating magnetic axis to external fiducials	
Q1 Displacement transverse	300 µm	Within limits, correctable if adjustments made to cryostat jacks, if fiducials are stable. Mechanical tests scheduled for 2001		150 µm
Displacement longitudinal	~1mm			
Roll angle	200 µrad (rms)			100 µrad (rms)
Pitch/Yaw				130 µrad
Q2 Displacement transverse	300 µm			150 µm
Displacement longitudinal	~1mm			
Roll angle	100 µrad (rms)			100 µrad (rms)
Pitch/Yaw				130 µrad
Q3 Displacement transverse	300 µm			150 µm
Displacement longitudinal	~1mm			
Roll angle	100 µrad (rms)			100 µrad (rms)
Pitch/Yaw				130 µrad

FIG. 6: Reference alignment table for the LHC IR inner triplet magnets.

must go toward the development of such quadrupoles since the optics requirements for a doublet flat optics call for a 2-in-1 doublet, where the apertures are vertically separated by only a few centimeters. A further constraint to the design is the fact that the neutral debris from the IP would hit the conductor in a traditional 2-in 1 design. Alternative designs based on modified Panovsky quad are presently being explored at BNL (see Figure 8).

A very aggressive R&D schedule could have a short model by FY12-FY16, with the cost of R&D depending on the outcome of R&D on HTS or alternative materials.

IR Separation dipoles for VLHC-2 Stage 2 require very high field, 12-16 T. R&D issues are similar to IR quadrupoles: design, fabrication technology, field quality, quench performance, cooling, quench protection. The R&D goal is a short model by FY12-FY16.

R&D for all VLHC IR magnets, VLHC-1 and even more so, VLHC-2 will require a consistent underlying R&D effort in super-conducting magnet cable technology, and magnet design. Considerable effort will be required in developing magnet design program adequate to realistically predict magnet performance and field quality for non-traditional magnet designs.

E. IR correction and feedback systems

Correction is a critical aspect of IR design for future colliders, given their potential to allow a more cost effect design by relaxing stringent requirements on IR parameters and to improve operational performance. The main performance limitations, discussed above are recalled in Table IV with the associate correction system.

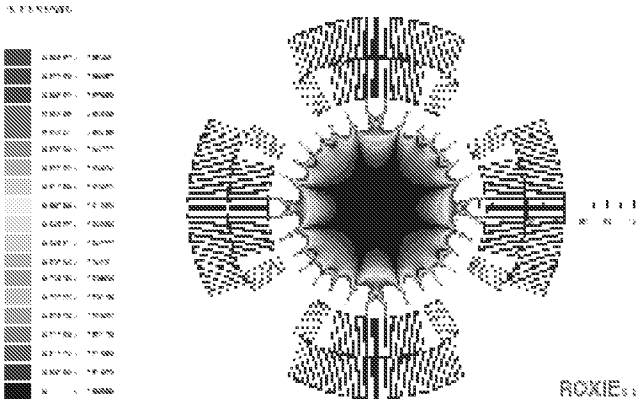

FIG. 7: Cross section of a Nb3Sn IR magnet design for VLHC Stage 1

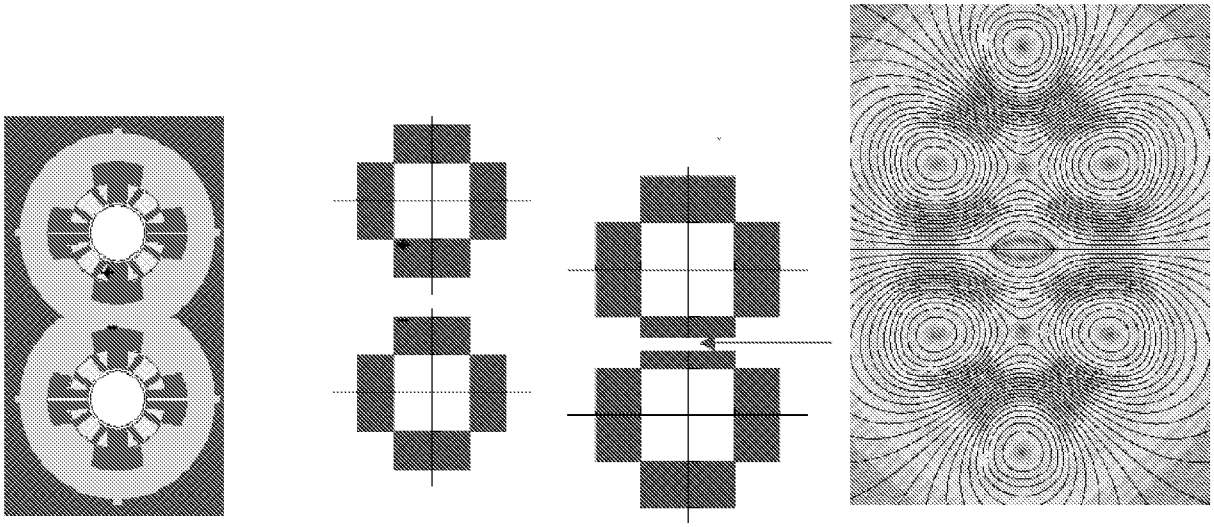

FIG. 8: Cross-section of, respectively, a traditional 2-in-1 design, a Panovsky-type quadrupole and a modified Panovsky quadrupole to remove the conductor from the mid-plane. The right most picture describes the field generated by a modified Panovsky quadrupole, a possible candidate for a 2-in-1 doublet for VLHC Stage-2 (flat beam optics).

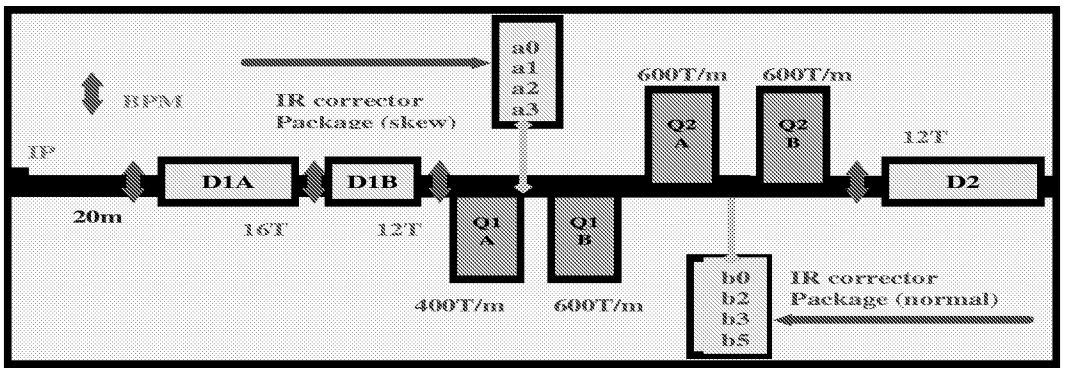

FIG. 9: Schematics of IR correction for the VLHC-2, flat beam optics, with the skew correction layers next to the defocusing quadrupoles and the normal layers next to the focusing quadrupoles.

TABLE IV: IR performance limitations and associated correction system.

IR performance limitation	*Correction system*
Long range beam-beam tune shift	Beam-beam compensation schemes
IR final focus magnets field quality	Local IR linear and nonlinear correctors
Alignment, stabilization	Orbit and IP feedback

A program for beam-beam compensation is underway at the Tevatron and alternative schemes to compensate long-range beam-beam effects with a wire across the IRs are presently being explored at the LHC.

Local IR correction packages next to the IR triplets are integral part of the RHIC IR design and the scheme with some modification was adopted for the LHC and the VLHC design. Packages that contain linear and nonlinear multi-layer correctors are placed next to the IR final focus magnets to compensate locally the field errors in the triplet and separation dipole magnets. Figure 9 describes the proposed layout for the VLHC, based on the experience from RHIC and the LHC and the projected field errors.

The IR correctors have been used at RHIC to operationally correct locally the coupling effect arising from the IR triplets and work has started on local compensation of nonlinear effects. Coupling in the IRs arising from IR quadrupole misalignment has been an operational issue for the Tevatron; in RHIC the local correction of coupling allowed to reduce the strengths of the skew families compensating globally for the coupling resonance and helps controlling coupling effects during the ramp. Local nonlinear correction is expected to be useful during the process of beta squeeze for RHIC and the LHC, when the transverse beam dimensions become large with respect to the good field aperture in the IR triplets, and in the VLHC to mitigate the effect of closed orbit offsets and crossing angle in the final focus quadrupoles.

For the VLHC, where the transverse beam dimensions are negligible in comparison with the pipe radius and the magnet apertures, the control of the closed orbit, tunes and chromaticity becomes more important than dynamic aperture considerations, traditionally considered the ultimate figure of merit for collider performance. Alignment and mechanical tolerances can be relaxed by planning and integrating feedback systems in the IR design from the start. Feedback techniques developed for e+e- colliders can be useful and applicable to hadron colliders IRs.

It has been the consensus at the workshop that the main R&D effort for the development of IR system for hadron colliders in the foreseeable future is the experimental verification of the predicted performance limitations and the proposed IR correction schemes. We propose a collaborative experimental program in the next 3-6 years at existing hadron colliders, RHIC, the Tevatron and later on LHC in the following areas:

- Measurement of beam-beam effects, long range and coherent modes respectively to verify performance predictions for the LHC and the VLHC
- Experimental verification of beam-beam compensation schemes
- Local operational IR correction, linear and nonlinear
- Test of closed orbit, tune and chromaticity feedback systems to relax IR requirements

A first phase of beam experiments will exploit the natural machine development activities at the existing machines, while in the second phase (3-6 years) larger dedicated collaborative experiments should be planned at existing facilities to systematically explore parameters of interest to future hadron colliders.

A coordinated program of collaborative beam experiments can be the ideal test bench for the technical and sociological challenges of GAN (Global Accelerator Network): a success in distributed beam experiments among institution would be a proof of principle for the concept of running an accelerator from control rooms distributed around the world. We estimate that 2-3 FTE's per collaborating laboratory should be enough to develop and implement a plan for collaborative beam experiments R&D.

F. Energy deposition and background

Energy deposition in the IR components is a big challenge for the planning of future hadron colliders. For the LHC, ~900 Watts/side of debris is generated at nominal luminosity and energy. Of this ~200 Watts that would otherwise hit the first IR quadrupole is intercepted by an upstream absorber, and another 200 Watts is deposited in the cryogenic system through the beam tube and beam tube liner. Aside from the cryogenic load, some of this debris can interact directly with the magnet, raise the magnet temperature and cause a quench. The radiation in the long term can degrade the magnet components (for example 7 years of LHC operation translates into 20 MGy, which causes the epoxy in G-11CR to disintegrate) and cause activation of magnets and shielding.

Simulations of energy deposition have been done for the LHC IRs, that show that the heat load distribution have longitudinal, radial and azimuthal dependence, besides the natural functional dependence on energy and luminosity.

The debris from the IP rises to 3 KWatts/side at VLHC-1 and 24 KWatts/side at VLHC-2. With a factor 3 between the LHC and VLHC-1, an extrapolation of energy deposition effects and cures is reasonable. Extrapolation no longer works for the VLHC-2. An initial evaluation of energy deposition and backgrounds in the IR components has started for the VLHC-2, but more needs to be done. The R&D program needs to address the following:

Modeling of energy deposition effects and background effects (MARS, PHYTHIA)

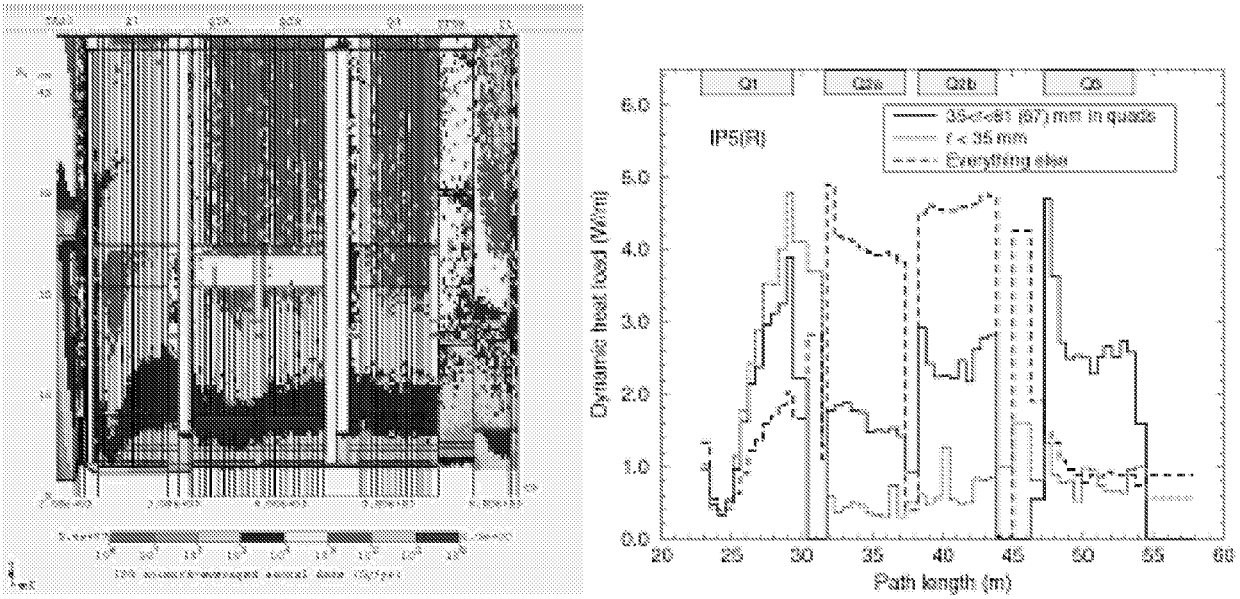

FIG. 10: Heat load distribution in the LHC interaction region triplet area.

Design of an IR components protection systems, that must include collimators, liners, absorbers and inner absorbers, and active cooling of components

Use of superconductors with larger temperature margins and radiation resistant materials.

G. Integration of accelerator and experiments

For the IRs of future hadron colliders, the accelerator and the experiments need joint planning to optimize the physics output of the machine and the engineering layout of the interaction regions.

Aspects that determine the physics output are the lengths of the luminous region, bunch crossing time, energy and luminosity. A short luminous region is called for by the requirement of reconstructing the missing E_t, a long one allows for simpler vertex reconstruction and lowers the radiation damage. Stability during the store is essential at the VLHC, calling for IP feedback. Having a small number of interactions per crossing eases the event reconstruction and that can be achieved by reducing bunch spacing. Below 20nsec, however, with the present technology, events will not be resolved by the detector, the limit being detector components (phototubes, silicon, etc.) which have response time of ∼10 nsec, due to physical limits on charge collection and integration time, with only Cherenkov devices at the moments having response time of the order of 4-5 nsec. A detector R&D program is needed to increase detector response or deal efficiently with multiple interactions, to optimize the accelerator output.

The other area where integration between accelerator and experiments is quite natural and essential is in planning the IR layout, mechanically and functionally. The energy deposition and background challenges will require that the interface elements merge, following the example set by the development of the HERA IR upgrade program. Multi function devices, active beam pipes and active absorbers (an example the TAN detector at the LHC) will be needed, shielding around the beam pipe to reduce IP background and shielding after the final focus magnets to reduce machine background. There is confidence that such systems can be built for VLHC-1, while more effort will be needed for planning of the VLHC-2.

Critical areas of experiment R&D that impact the machine are radiation hardness, detector resolution and granularity. More specific joint experiment-accelerator R&D is needed in the development of multi function components, (active beam pipes and absorbers), combined function IR magnets, and joint use of IR devices (as an example the first separating dipole in a flat beam optics could be use a s a spectrometer, etc.

III. LEPTON-HADRON COLLIDERS

The working group reviewed the interaction region design and issues existing and planned lepton-hadron colliders, namely HERA and its IR upgrade, eRHIC, EPIC and finally THERA.

Matching the machine to the physics to be studies is fundamental for lepton-hadron colliders, so energy tunability, flexibility in selecting the ratio of lepton and hadron energy, ion species and availability of polarized beams are fundamental. Small emittance is important, as is small divergence, so a trade-off between these requirements and luminosity may be the best option here. The conclusion is that from the physics point of view a low emittance 4-10 GeV polarized electron linac at RHIC is the best project for a e-hadron collider.

The HERA IR upgrade is a very useful example guiding the design of e-hadron IR colliders. The main issues have been the development of special IR magnets (large aperture, placed inside the detector, with holes for the other beam, necessitating good field quality and correction coils attached to the magnet itself). To reach and monitor the alignment requirements a stretch wire system developed at the FFTB was used to measure displacements with 1 μ resolution and roll angles. Background and synchrotron radiation were reduced to acceptable level by masks and carefully threading of the beam through the detector.

An IR design for the THERA interaction region has been developed, the main issue is obtaining reasonable luminosity (the present design figure is 3 orders of magnitude smaller than HERA), the biggest obstacle being the mismatch between the small Tesla electron beam size and the HERA proton sizes. Cooling of high-energy proton beam does not appear very promising.

General issues about e^-hadron interaction regions, and related R&D, were identified and addressed at a round table on this subject. The main issues discussed have been the luminosity, the determination of the collision frequency, the interface between accelerator and experiments, head-on collisions versus crossing angle, synchrotron radiation and backgrounds and finally, the energy range. The main areas were R&D is necessary are a systematic study for the optimization of the collision frequency, development of special final focus magnets, the development of a 4π detector, control of beam halo and electron cooling for proton beams.

IV. E^+E^- LINEAR COLLIDERS

A. Introduction

The Interaction Region Working group reviewed the Interaction Region systems of the proposed e^+e^- Linear Colliders, including TESLA, NLC, JLC and CLIC. One session was also devoted to discussion of the $\gamma\gamma$ collider. The primary challenges for a linear collider IR are the control of backgrounds and the design and support of the final quadrupole doublet. The backgrounds arise both from the incoming beams and from the beam-beam interaction, the latter of which are proportional to the luminosity. The design of the extraction line is also an issue as is the instrumentation to measure beam quantities required for either the experiment or the operation of the accelerator.

B. IR layouts

Layouts of the IR region integrated with the proposed detectors have been developed for JLC, NLC and TESLA. As shown in Figures 11, 12 and 13, all of the IRs are similar, but the plan views for NLC or JLC differ from TESLA due to the crossing angle and separate extraction line. All designs use tungsten shielding, instrumented masks, and low Z material to absorb low energy charged and neutral secondary backgrounds. Future R&D will include increasingly detailed simulations as the design of the interaction region and detectors mature.

Figure 11 shows the plan view layouts of the NLC interaction region for a 3T Large Detector model (on the left) and a 5T Silicon Detector model (on the right). The crossing angle is 20 mrad and the distance from the IP to the nearest quadrupole magnet (L^*) is 3.8m. The Sm_1Co_5 permanent magnets are sized to produce the gradient for 250 GeV beams with a 1 cm radius aperture. The relative angular acceptance of the ECAL/M1/LUM system is determined by the detector solenoid field, the 60 cm minimum overhang of the instrumented W-Si M1 mask, which protects the detector from the secondary particles backscattered from the Luminosity/Pair Monitor, and the 1cm radius exit aperture of the LUM. For the Large Detector these are 52-mrad/32-mrad/6.3-mrad, respectively; for the Silicon Detector the equivalent acceptances are 156-mrad/30-mrad/6.3-mrad. The difference in ECAL acceptance for LD and SD is simply due to the fact that the starting z locations for the two designs are 3.0m and 1.5m, respectively, while the M1 mask outer dimension is about the same. From a practical point of view, the major difference in the two design choices is that for the Silicon Detector the LUM and closest magnets are further from the endcap calorimeter front face. This permits a longer and thicker M1 mask and thus better shielding from backgrounds. In SD most of the QD0 magnet is outside the region of the magnet yoke, which ends at 4.2m. This means that deleterious effects of the fringe field on the permanent magnet are minimized. Outside the detector, magnet mounting is easier and there will be

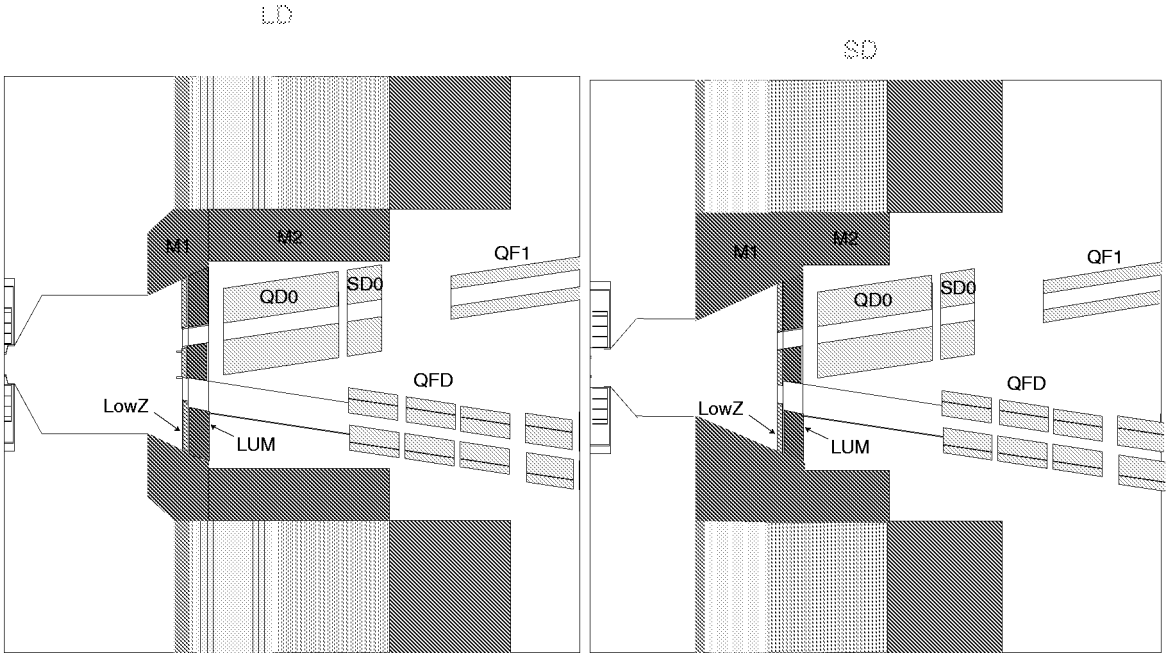

FIG. 11: Plan view layouts of the NLC interaction region for the 3T Large Detector model (left) and the 5T Silicon Detector model (right).

more space to consider alternative magnet technologies that may need more space. Furthermore, the extraction line, which begins at 6m from the IP, is well outside the detector. As most of the high energy pair particles are lost near its front face, the resulting photons find it more difficult to reach the calorimeters. For the LD, the photon backshine sees both the endcap ECAL and HCAL, and the M2 mask must be thickened to protect the innermost layers from backgrounds.

Figure 12 shows the layout of the TESLA interaction region which has no crossing angle. The detector solenoid field is 4T. The closest magnet to the IP is a SC quadrupole at an L^* of 2.75 m. The back end of the luminosity monitor is at 2.4 m. The instrumented conical mask subtends the region from 27.5 mrad to 83.1 mrad. The pair luminosity monitor provides acceptance below 27.5 mrad. Graphite absorber placed in front of the LUM-PAIRMON helps to stop soft albido produced by the pair interactions.

Figure 13 shows the layout of the JLC interaction region. This design uses an 8 mrad crossing angle. The beam is extracted through the coil pocket of a normal iron quad protected from the 2-3T detector solenoid field by a SC compensation magnet.

C. Background issues

At the proposed IP beam parameters for 500 GeV, the IP background of most concern is the incoherent production of e^+e^- pairs. The number of pairs produced is approximately proportional to luminosity and is similar for the TESLA and NLC designs. GuineaPig simulations indicate that 1-2 $\times 10^9$ e^+e^- pairs will be produced per second with an average energy of 25-30 GeV. GEANT and FLUKA based simulations indicate that detector occupancies in the relevant readout time (per bunch, per train, or per readout time) are adequately low. Neutron production by the pairs dominated the radiation dose to the vertex detector; with the current layouts, the lifetime of a CCD-based vertex detector is estimated to be some number of years.

Figure 14 shows the calculated charged particle and photon hit densities for the NLC Large Detector (3 Tesla field). The plots include the contributions from the production of e^+e^- pairs that interact directly in the detector and from their secondary debris. For 1.2 cm $< r <$6.0 cm, the charged particle hit density per 190 bunch train is plotted for the vertex detector at 500 GeV and 1 TeV c.o.m. The hit density rapidly drops from the 10 hits/mm^2/train level at the first layer of the VXD and should not cause any problems in pattern recognition. For r>10 cm the average photon density, before conversion, is plotted. Typical conversion efficiencies are in the range of 1-2%. As is evident in Figure 15 the photons come from the central region of the detector where pairs hit the beam pipe, and from the faces of the closest piece of high Z material. In NLC's case these are the extraction line magnet at 6m and the front end of the LUM at 3.5m. The density is calculated

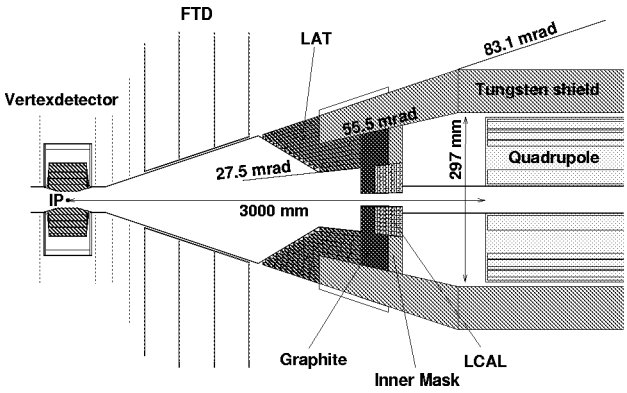

FIG. 12: Layout of the TESLA interaction region.

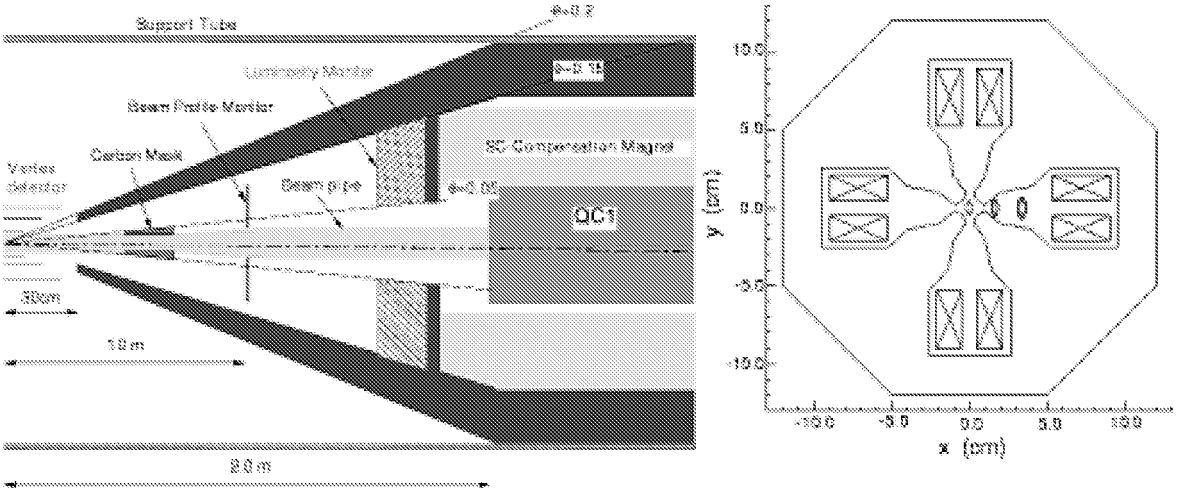

FIG. 13: Layout of the JLC interaction region.

for a fixed tracking chamber acceptance of $\cos\theta = 0.92$; this accounts for the somewhat counter-intuitive falloff as r increases. Similar plots for the 5 Tesla NLC Silicon Detector show hit densities that are roughly a factor of two smaller.

Figure 15 shows the corresponding background estimates for the TESLA detector and beam parameters. The left plot records the absolute number of hits due to the production of e^+e^- pairs and their secondary interactions in the vertex detector, layer by layer, for 500 GeV and 800 GeV c.o.m. energies and two possible values of the solenoid field. The right plot shows the number of photons in the TPC as a function of z for the two beam energies. The results are shown here for one bunch crossing so the final detector occupancy will depend upon the integration time of the readout.

D. TESLA Superconducting Linear Collider

1 Crossing angle

The 337 ns bunch-to-bunch separation in TESLA allows for a zero crossing angle at the IP without introducing unwanted parasitic collisions. The exiting beam is swept away from the incoming beam to a separate charged particle dump by electrostatic separators located 50 m from the IP. The zero crossing angle has several advantages which simplify the IR layout but which make the beam extraction and diagnostics more difficult. The final quadrupole doublet is on axis with the detector and its solenoid field and there are no perpendicular components of the solenoid field to complicate the optics. The detector acceptance is azimuthally uniform and the geometry of the innermost detector elements cylindrically symmetric. The bunches collide head on and there is no need for transverse RF ("crab") cavities to rotate the bunches. The TESLA design also has a superconducting quadrupole doublet which provides flexibility for operating at different beam energies. The

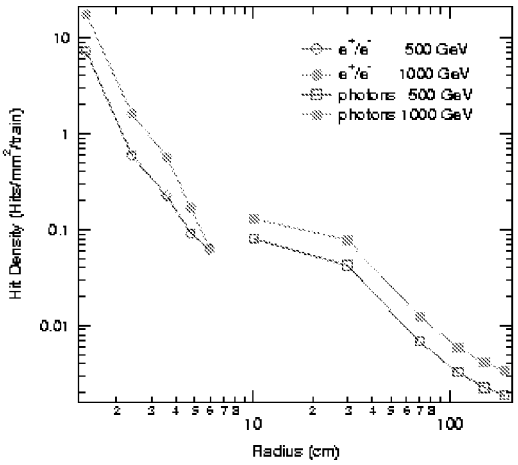

FIG. 14: Tracking chamber backgrounds due to e+e- pairs in the NLC Large Detector.

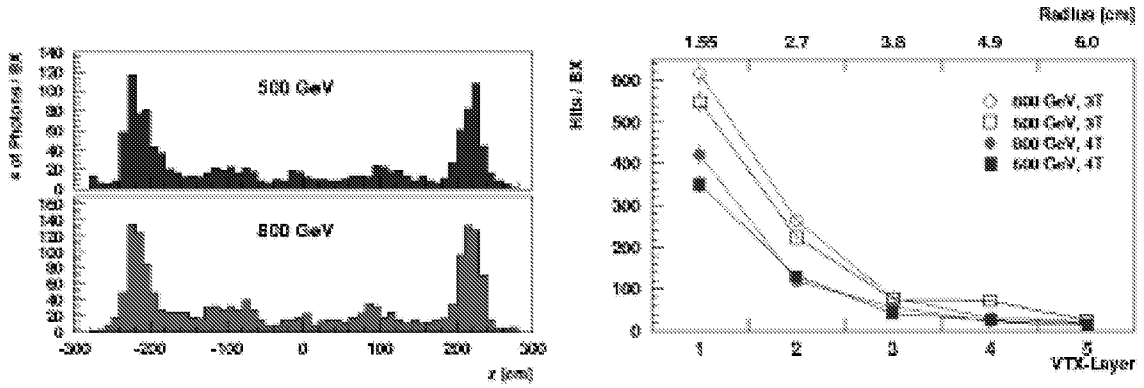

FIG. 15: Background estimates for the TESLA detector.

disrupted beam is extracted through the large bore of the quadrupoles so that transverse space need not be found for a separate extraction line magnet system and there is a large aperture for the passage of halo-induced synchrotron radiation. Engineering studies of the TESLA SC quadrupoles are based on similar LHC magnets, as shown in Fig. 16.

The lack of a separate extraction line necessarily complicates beam disposal and the placement of diagnostic instrumentation downstream of the interaction point. Fig. 17 shows the layout of the TESLA beam lines in the vicinity of the interaction point. The outgoing beam is bent away from the incoming beam via an electrostatic septum which must be shielded from beamstrahlung photons and other radiation. There is sufficient power deposited in the vicinity that, in the current working design, there is no suitable location for diagnostics such as the polarimeter and energy spectrometer, downstream of the interaction point. While these can nominally be located upstream, that solution precludes measurement of the polarization after the beam-beam interaction. While the expected depolarization due to beam-beam effects is small, there is concern that systematics will limit the achievable accuracy of the polarization measurement. There is also concern that the off-energy electrons created through the Compton process at an upstream polarimeter can create additional beam backgrounds, and this must be simulated and understood. Since the charged particle beam is directed to a primary beam dump which is off-axis with respect to the detector, there is an advantage that the vertex detector will not be in the direct line of sight of the dump window. However, a separate high power dump is required at zero degrees for the beamstrahlung photons that carry off roughly 10% of the beam energy. As a final consideration, the most likely path to next-generation higher energy collisions is believed to be higher frequency RF accelerators with very short bunch-to-bunch spacing which require a crossing angle, such as CLIC. A linear collider where the linac tunnels do not have an adequate crossing angle would not be suitable for an upgrade to higher energy with these technologies.

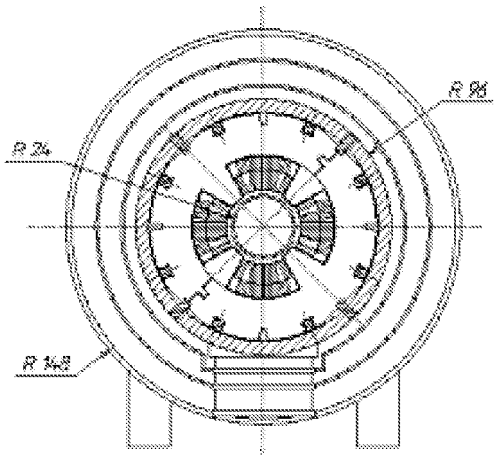

FIG. 16: The TESLA SC final quadrupole, based on the LHC final quad design.

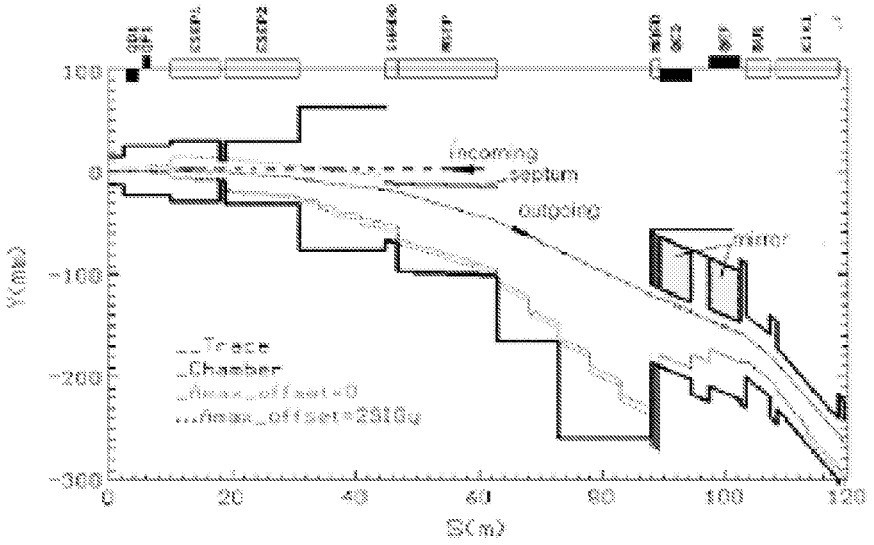

FIG. 17: Layout of the TESLA beamline near the interaction point.

2 Disruption enhancement and IP feedback

The current TESLA IP parameters include on a relatively large luminosity enhancement factor of 2.1 from beam-beam disruption. This enhancement degrades rapidly to unity as the beams are offset. Figure 18 shows the sensitivity of TESLA luminosity to vertical displacement of the beam. An offset of $0.1\sigma_y$ causes a 2% reduction in peak luminosity.

This sensitivity to offset implies tight constraints on vibrational stability which must be maintained in the face of naturally occurring ground motion and laboratory-produced sources of vibration, such as pumps and compressors, perhaps accentuated by mechanical resonances in either the quadrupole doublet itself or its support inside the detector. In the TESLA design, constraints on the jitter of the final doublet magnets are mitigated through the use of an intra-train feedback system. Simulations indicate that such a system can have sufficient bandwidth and sensitivity to correct motion to the required $0.1\sigma_y$ level.

Fig. 19 shows the intratrain feedback system design and its performance. The large beam-beam deflection that occurs when the beams to not collide head-on allows for an accurate determination of the beam offset with modest BPM resolution. With a large inter-bunch spacing of 337 ns, there is adequate time to allow digital processing of the correction algorithm. The left part of the figure shows the layout of the BPMs and correcting kickers as well as a plot of the beam deflection versus beam offset. The right side of the figure shows how the algorithm can correct for even large displacements of the bunch trains after sampling only a small fraction

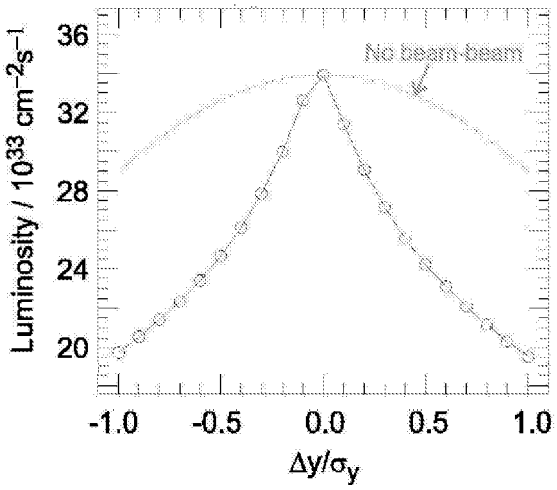

FIG. 18: Sensitivity of TESLA luminosity to vertical displacement of the beams. The relatively large luminosity enhancement factor of 2.1 due to disruption degrades rapidly as the beams are offset.

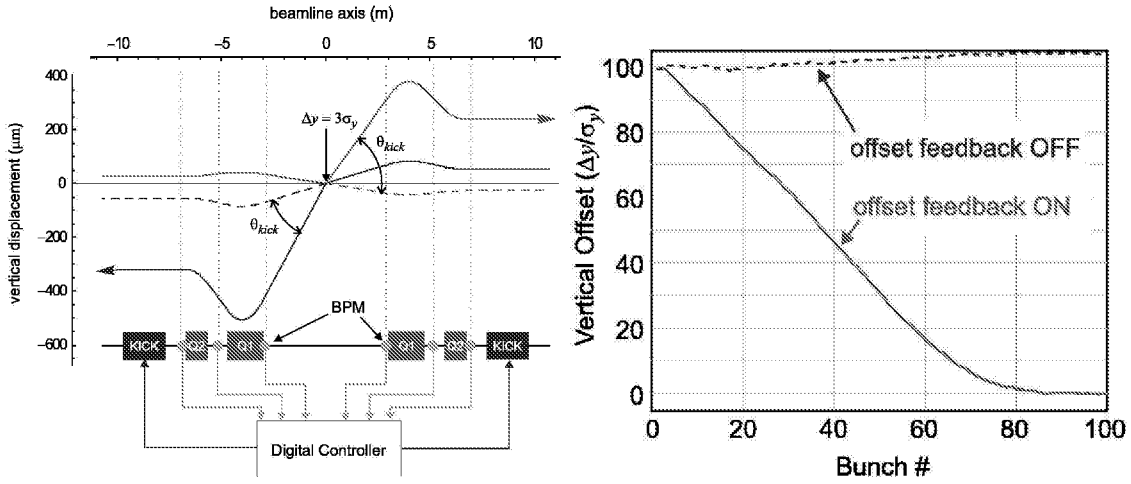

FIG. 19: Layout of the TESLA intra-train feedback system and a simulation of its performance.

of the 2820 bunches in a train. A similar system is forseen to correct for angle offset. The feedback system has been simulated in detail and prototype units have been tested at TTF. This gives confidence in its design and performance, assuming that the bunches in each train are uniformly displaced and have identical charge distributions. Disturbances that might affect each bunch independently, such as damping ring extraction kicker jitter combined with some $x - y$ coupling of the beam, would not be removed by this system.

E. NLC/JLC X-band Linear Collider

1 Crossing angle

An X-band linear collider with an inter-bunch spacing of 1.4 ns requires a crossing angle of at least 3-4 mrad to avoid parasitic beam collisions. A larger crossing angle provides more space to accommodate a separate extraction line but requires crab cavities to limit the luminosity loss due to the relative rotation of the two colliding bunches. The maximum crossing angle is limited by the accuracy to which the crab cavities can be synchronized. If the luminosity loss is required to be less than 2%, this sets a tolerance on the relative phase of the two crab cavities. From engineering considerations, a reasonable limit appears to be of 0.1 degrees of relative phase difference at X-band or 0.025 degrees at S-band, which translates into a maximum crossing angle of about 40 mrad.

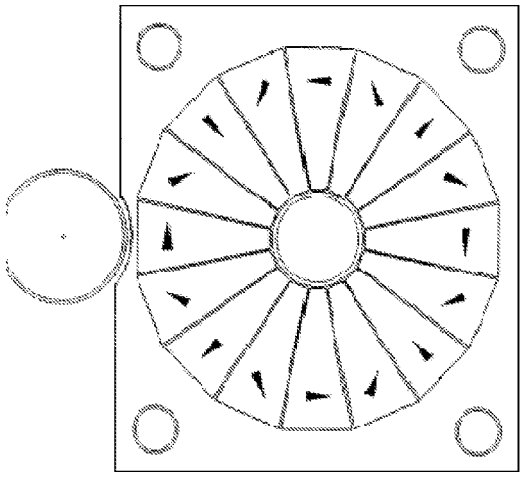

FIG. 20: Cross-section at L* of the permanent magnet quadrupole being currently considered for NLC.

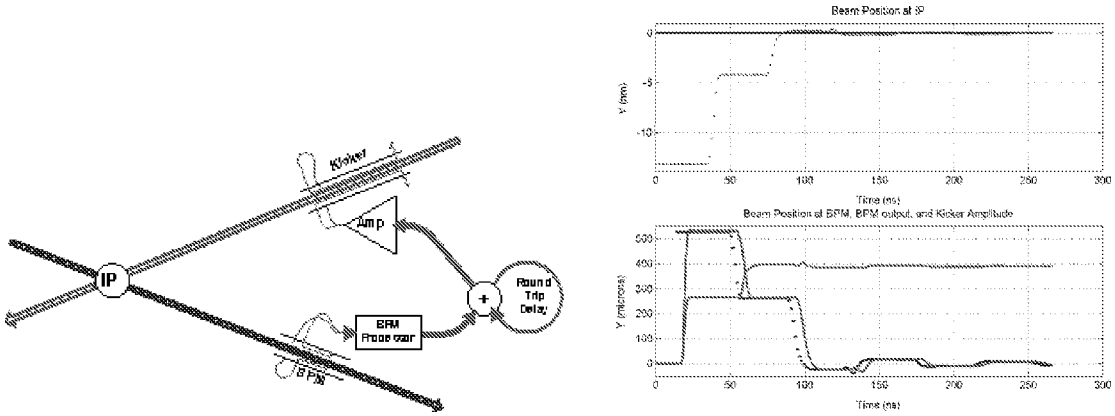

FIG. 21: Scheme and simulated performance of intratrain feedback at the NLC.

The JLC collaboration has chosen a crossing angle of ±4-mrad, on the low side of the range, in order to relax the requirements on the crab cavity system, or to eliminate it entirely. With this choice, the extracted beam is required to pass though the coil pockets of the conventional iron magnets of the final doublet that focuses the incoming beam, as shown in Figure 13. The choice of conventional iron magnets necessitates the use of a superconducting flux-exclusion tube to shield the magnet from the detector's solenoid field.

The NLC collaboration, more confident in the crab cavity system performance, has currently chosen a crossing angle of 20 mrad. This provides enough transverse separation between the incoming and outgoing beams to allow completely independent magnet systems for each beam, as long as the magnets are transversely compact. The baseline NLC design assumes the use of compact permanent SmCo magnets, which could provide both the required gradient and aperture in the space allowed. Additional advantages of using permanent magnets lie in the fact that they can be made mechanically stiff and light, and can be detached as much as possible from the vibrationally-noisy external world of power supplies and cooling systems.

Figure 20 shows the cross-section at L^* of the permanent magnet quadrupole currently under consideration for the NLC. The quadrupole is of the Hallbach type, composed of 16 wedges of magnetized SmCo encased in a stiffening frame of carbon fiber and non-magnetic structural beams to keep it as light and rigid as possible. It is desired that internal vibrational modes be of sufficiently high frequency that they not be excited by typical 60 Hz vibrational noise sources. The magnet would be free of external connections that might couple in external vibration sources and would not require cooling water, another potential vibration source. With the current NLC final focus optics the inner diameter of the magnet is 2.0 cm and the maximum external dimensions are set by the size of the beam pipe needed for the extracted beam.

The extraction line lattice begins at 6-m from the IP, but the beam pipe must be large enough to accommodate the entire cone of beamstrahlung radiation. The required stay-clear is set at 1 mrad, 5-6σ times the *rms* angular

distribution of the photons. This translates into a 1-cm radius aperture at the back end of the extraction line quadrupole doublet at ~10 m. In figure 20 the extraction line beam pipe is on the left and has a 1 cm diameter at L^* while the incoming beam pipe aperture is that from an earlier optical model that assumed shorter, stronger magnets and a 0.6 cm radius incoming aperture. The figure shows that even with a 20 mrad crossing angle, care is needed in the design to have everything fit together without conflict.

A possible problem with the permanent magnet technology choice would seem to be a lack of tunability of the final doublet strength. Recent discussions with the user community have indicated a desire for fairly frequent and rapid changes in beam energy, which would require proportional changes in the integrated field strength of the doublet. In principle, counter-rotating segments at the rear end of the magnet could provide strength variation in a permanent magnet system. In practice, however, this solution seems unwieldy and antithetical to the light-and-stiff design philosophy.

An exciting alternate possibility came out of discussions with the magnet group *(T2)* at Snowmass. With the current state of the art, it is feasible to construct superconducting magnets with the required aperture and field gradient in the space provided. Since the Snowmass workshop, designs for both warm-bore and cold-bore magnets that meet all constraints have been developed [3]. While an SC magnet is inherently more flexible, there are concerns that the magnetic axis of a multi-layer superconducting magnet cannot be made stable against vibration at the required ~0.3 nm level. An R&D program to investigate the vibrational properties of superconducting magnets is planned, in addition to engineering studies of both permanent magnets, and compact SC magnet solutions for the final doublet.

Another possible problem with an IP crossing angle is the perpendicular component of the detector solenoid field seen by beams entering at ±10-mrad. This field can deflect the beams and cause them to miss each other, and dispersively increase the spot size due to the finite energy width of the beam. It has been shown [4] that simple beam steering with upstream optical elements and slight offsets of the final doublet will bring the beams back into collision and simultaneously nullify any dispersive effects on the beam spot size. In principle, one must also consider the Oide effect, which is the increase in the spot size due to the emission of synchrotron radiation in the field, an irreducible contribution proportional to $(L^*\theta_C B_{sol})^{5/2}$. This has most recently been calculated for the NLC "small" detector with $B_{sol} = 6$ Tesla and $L^* = 2$ m and shown to be negligible. Attention needs to be paid to changes in the IP layout that may increase this product.

An important advantage of the crossing angle is that it allows a separate extraction line for better control of the disrupted beam. For NLC, an extraction line lattice has been developed [5] that transports the charged beam and the neutral beamstrahlung photon beam to a common photon-electron beam dump. The magnet apertures are sufficiently large to pass the disrupted beam and its low energy tail with minimal beam loss. A chicane is used separate the charged and neutral beams, to provide a location for diagnostics. An SLC-like polarimeter would be located in this region, along with possibly other energy and polarization diagnostics. More discussion and design work from the user community is required to develop detailed plans for this equipment.

2 Disruption enhancement and IP feedback

For the NLC, the luminosity has a sensitivity to vertical displacement which is similar in shape to that shown for TESLA in figure 18 but is smaller in magnitude. A 2% luminosity loss would require a displacement of $\sim 0.3\sigma_y$, or about 1-nm. As mentioned earlier in the discussion of magnet technology choices, the primary solution to final doublet jitter problems are passive. That is, the interaction region geology, the detector in which the magnets are mounted and the mechanical design of the quadrupole supports must all be chosen or designed to minimize magnet jitter and its transmission. Care must be taken to avoid introducing vibrations from pumps, compressors and other moving machinery, by locating them a suitable distance from the IP, providing mechanical isolation, and engineering for low vibration. It is also important to minimize or eliminate cooling circuits and cabling which attach the magnet to potentially noisy service areas.

Any jitter not passively eliminated will be dealt with through a combination of active sensors, magnet movers, and correctors in either open or closed feedback loops. Additionally, an analog variation of the intra-train feedback foreseen for TESLA, operating with 40 ns latency, can effectively correct any residual jitter up to $\sim 15\sigma_y$ for the trailing 80% of the 266 ns bunch train. An extensive R&D program in ground motion measurement, inertial and interferometric sensor design, actuator performance, and feedback algorithm development has already begun to demonstrate proof-of-principle solutions to the magnet jitter problem. Tests on realistic, mechanical mockups of the IR are scheduled for FY2003-04.

The left side of figure 21 depicts the intratrain feedback scheme currently under consideration for the short intrabunch spacing of the warm RF accelerators. The beam deflection due to a relative offset of the two beams is measured by a BPM located near the interaction point. The correction signal is rapidly processed and fed to a electrostatic kicker that corrects the position of the oppositely charged bunch train. Correcting the opposite

beam avoids the time of flight delay of sending a signal across the detector and is equally effective for relative offsets of the beams. The feedback loop is closed and deflection minimized in a time dominated by the time of flight between the kicker/BPM and the IP.

Simulations using plausible values for the time of flight delay, electronics processing time, and system gain have shown [6] that much of the otherwise lost luminosity can be recovered. More recently, a realistic design for the analog electronics has been completed using only off-the-shelf components [7]. Parts of the circuit have been prototyped and the performance of the system calculated using the SIMULINK electronics performance tool, with a beam-beam deflection curve predicted by Guinea-Pig as input. The right hand side of figure 21 shows the capture transients from an initial beam-beam offset of $5\sigma_y$ (13 nm). The upper part of the figure shows the vertical position of the beams at the IP. The lower plot shows the position of the outgoing beam at the BPM (blue), the analog response of the BPM processor (green), and the kicker drive signal, in arbitrary units, in red. Essentially full luminosity is recovered in 80 ns. The actual response of the circuit can then be used within Guinea-Pig to estimate the luminosity loss [8]. An uncorrected luminosity loss of 60% for the $5\sigma_y$ offset depicted in the figure is reduced to 10% with the feedback system. At $15\sigma_y$ initial offset an uncorrected loss of 90% would be reduced to 30%. A test of a prototype circuit is planned in the NLCTA in early 2002, using a $\sim$200 ns train of low energy pulses bunched at 11.4 GHz. This will measure the effectiveness of the circuit in an accelerator environment where practical concerns of noise, radiation, electronic drift can be evaluated.

3 Final doublet stabilization

To achieve the required nanometer stability of the final doublets with respect to each other, some kind of inertial stabilization system will likely be required. Two different approaches are to stabilize the final quadrupole doublet with respect to an inertial reference frame or with respect to the local bedrock that anchors the remainder of the beam delivery final focus system. Each solution has advantages and disadvantages. One may also choose to correct the beam motion itself with a fast dipole magnet in an open loop feedback, or to correct the position of the magnetic elements via movers in a closed loop feedback. Planned R&D studies span the range of possibilities.

Figure 22 shows an experimental setup designed to study the inertial stabilization in 3-dimensions of an object with no internal degrees of freedom [9]. The photograph to the left shows an aluminum block mounted on springs in a stand and equipped with accelerometers to detect block motion and electrostatic pushers to adjust motion. Data from the sensor array is read by ADCs, collected by a digital signal processor, and fed into a computer where a correction algorithm computes the required drive signals for each of the pushers in real time and applies it to the electrostatic pushers via a set of DACs. This provides a testbed for sensor types (accelerometers or geophones), sensor sensitivity and noise, actuator response, as well as the effectiveness of any given feedback algorithm. The right side of the figure shows the integrated RMS motion of the ground and the block in nm as a function of frequency under a variety of conditions. The curve of the mass motion with feedback off in the figure shows that the soft spring mounts damp the motion of the block relative to the ground above 10 Hz but create a resonance, as expected, at their natural frequency of $\sim$5 Hz. After the feedback is turned on, motion in this frequency range is also reduced to below the level of the ground. The lowest three curves on the figure are estimates of the residual motion after "slow feedback", based on the 120 Hz repetition rate of the beam, and various algorithms, are applied. It can be seen that with both of these types of feedback operating simultaneously jitter reduction across the entire frequency range to the few nm level is achievable. R&D in this area centers on improving the sensor and inertial algorithm. As a next step a system that looks at the relative motion of two blocks will be constructed. Later, more realistic long and slender magnet-like blocks, with internal degrees of freedom, will be studied.

It was suggested in the NLC ZDR [10] that the final quadrupole doublets be "anchored" to bedrock by using a Michelson interferometer to measure the motion of the magnets relative to the ground. Motion of the interference fringes would be detected by an array of photodiodes which would drive piezoelectric movers to correct the magnet motion in a closed feedback loop. Measurements have been done with a 1-m arm interferometer and zero-mass "magnet" (i.e. a mirror mount) [11] that show that the intrinsic resolution of the system is at the sub-nm level. Further tests with a 10-m long interferometer have given confidence that the arms in a practical setup will not need to be evacuated, but will need to be enclosed in tubes. One of the main drawbacks of this technique is the need to maintain clear lines of sight through the detector for the optical path. Recent R&D [12] has focused on extending the optical anchor technique to systems that ever more closely resemble actual magnets. Figure 23 shows a setup at the University of British Columbia for controlling motion of a reasonable mass with an optical system. In this case, for experimental convenience, horizontal vibration, either naturally occuring or externally induced with known amplitude and frequency, is controlled with the interferometer in a system which also tries to correct for real-life slow drift of the fringe pattern. The data on the right indicates how the position of the platform, (the red data points scattered between zero and 60 nm),

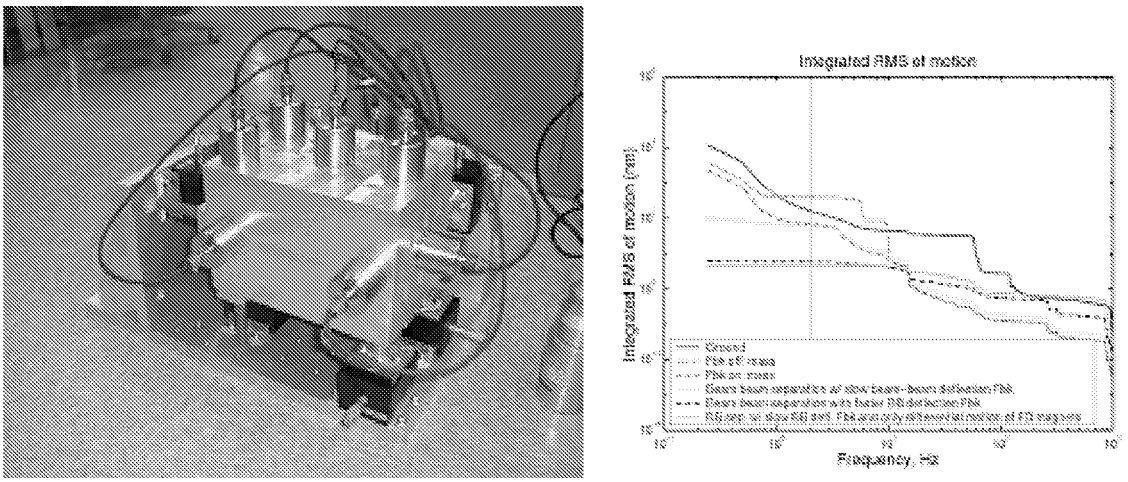

FIG. 22: Setup for inertial stabilization of the final quadrupole and results of the suppression achieved for a given set of suppression algorithms.

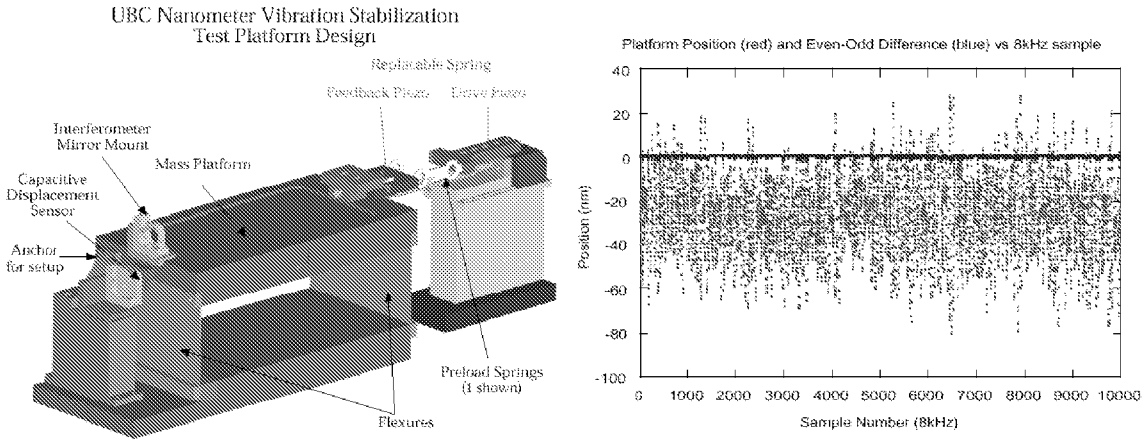

FIG. 23: The UBC setup for controlling motion of the final quad with respect to the local bedrock through interferometric means and a sample of data indicating the sub-nm resolution of the system.

is stabilized via the interferometer measurement to sub-nm levels (the blue points which appear as a thin line on the plot.) Future R&D plans follow the same path as that foreseen for the inertial program: ever increasing realism in the size and shape of the object stabilized and the use of the system to stabilize the relative motion of two magnets using the bedrock as a common reference platform.

A proposal has been formulated (the LINX proposal [13]) to reuse the SLC as an engineering test bed for final focus issues, especially those pertaining to collimation and final doublet stability. The proposal would replace the existing final quadrupole triplet with a doublet that incorporates "local chromatic correction" sextupoles. This, combined with some minor rewiring of existing magnets, could produce vertical beam sizes of 50-400 nm at the IP. With beams of the charge and size proposed, the beam-beam deflection signal is strong enough that relative beam motion at the 1 nm level can be measured by conventional BPMs with 1 micron resolution. Full scale engineering prototypes of any proposed system could then be tested using actual colliding beams well in advance of their need in an actual next generation linear collider. A study of the degree of effort and cost to revive the SLC vacuum, power, and control systems has been authorized and is in progress. If the LINX facility is eventually approved, several international collaborators have expressed interest in participating in what could be a very valuable engineering R&D tool.

V. $\gamma\gamma$ COLLIDERS

The possibility of a $\gamma\gamma$ collider has been dramatically increased because of recent progress in laser development and the engineering design of the IR optics that produce the γe collisions. The Mercury laser, developed at

LLNL for fusion applications, can serve as the demonstration prototype for the $\gamma\gamma$ collider laser. It will undergo full power tests by the end of FY2002. Conceptual designs are underway to take the 100-joule, 10-Hz output of the laser and match it to the time structure required for either NLC or TESLA. Large annular optics have been designed that permit the laser beams to be focused to the required 10-micron spots without putting any material in the path of the residual particle debris from the beam-beam collisions. Prototypes will be tested in FY2002. Independent laser and optics designs that profit from the longer interbunch spacing of TESLA are being evaluated. Changes to the final focus that decrease the horizontal spot size and increase the $\gamma\gamma$ luminosity are being developed.

VI. E^+E^- CIRCULAR COLLIDERS

The primary issues for the design of the IR for the high current dual ring e^+e^- circular colliders with small bunch spacing, such as KEK-B and PEP-II, are synchrotron radiation and beam pipe heating from trapped higher-order-modes. e^+e^- LCs share the need for SR masking, concerns about beam tail distributions, and orbit compensation due to the magnetic field of the detector. To increase the luminosity of the existing machines to $3x10^{34}$, the IRs will need to be modifies by replacing permanent magnets with higher field SC magnets and by introducing a small crossing angle. Figure 26 depicts a possible IR design for this luminosity incorporating a ± 3.25mrad crossing angle with extra SC quads indicated. An IR design for 10^{36} luminosity is in the conceptual stage.

VII. $\mu+\mu$- COLLIDERS

The IR design for a $\mu\mu$ collider is dominated by the shielding required to suppress backgrounds from μe decay. Many absorbers are required and, for optimal performance, their geometry must be configured appropriately for each machine energy. Figure 27 shows the shielding design for a 4 TeV muon collider on a highly anamorphic scale.

REFERENCES

[1] Design Study for a Staged Very Large Hadron Collider, VLHC Design Study Group, Fermilab-TM-2149
[2] J. Johnstone, Private Communication
[3] B. Parker, BNL, SLAC seminar, 10 Dec. 2001.
[4] P. Tenenbaum, SLAC, Snowmass 2001.
[5] NLC Extraction Line Studies, Y. Nosochkov and T. Raubenheimer, SLAC, LCC-0034.
[6] Simulations of an Intra-Pulse Interaction Point Feedback for the NLC, D. Schulte, CERN, LCC-0026.
[7] Design of an NLC Intra-Pulse Feedback System, S. Smith, SLAC, LCC-0056.
[8] P. Burrows, Oxford U., Snowmass 2001.
[9] J. Frisch, SLAC, Snowmass 2001.
[10] Zeroth-Order Design Report for the Next Linear Collider, LBNL-PUB-5424, SLAC Report 474, UCRL-ID-124161.
[11] M. Woods, SLAC, NLC Beam Delivery Meeting Notes.
[12] T. Mattison, U. of British Columbia, Snowmass 2001.
[13] Draft Letter of Intent for the LINX Test Facility at SLAC, The NLC Collaboration et. al., 7/15/01, http://www-project.slac.stanford.edu/lc/linx/papers/LINX_07-15-01.pdf

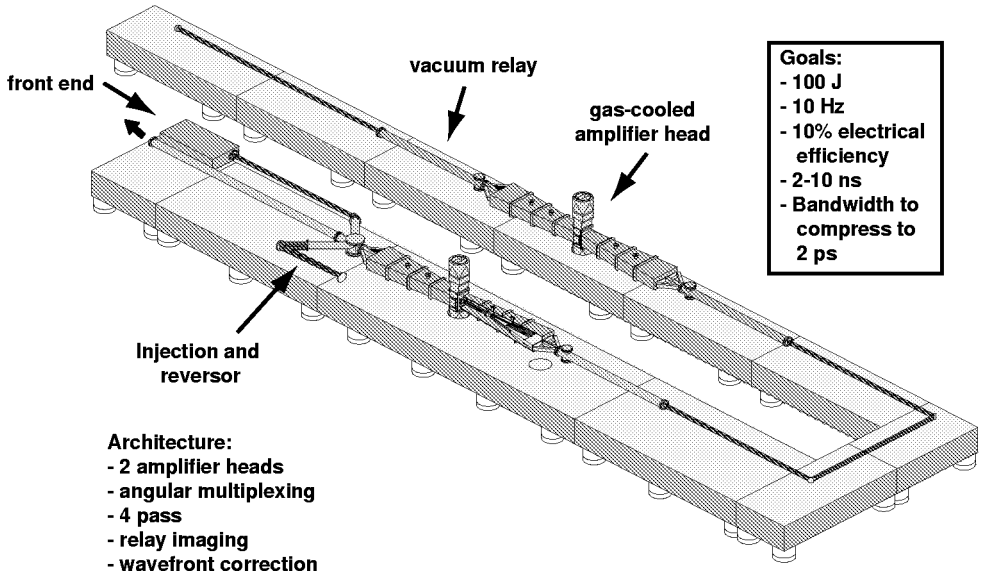

FIG. 24: The diode-pumped solid state Mercury laser is a high pulse rate, next-generation laser fusion driver.

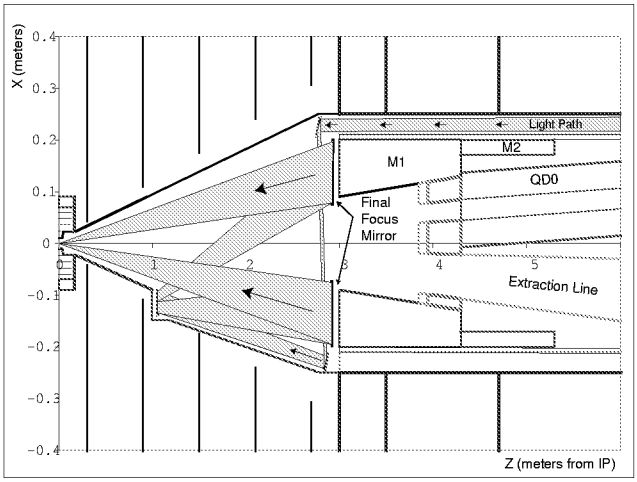

FIG. 25: The IR optical design of the $\gamma\gamma$ collider at NLC. A large annular mirror in front of the M1 mask and other mirrors placed out of the path of the beam bring the laser light into a 10-μm focus 5 mm from the IP.

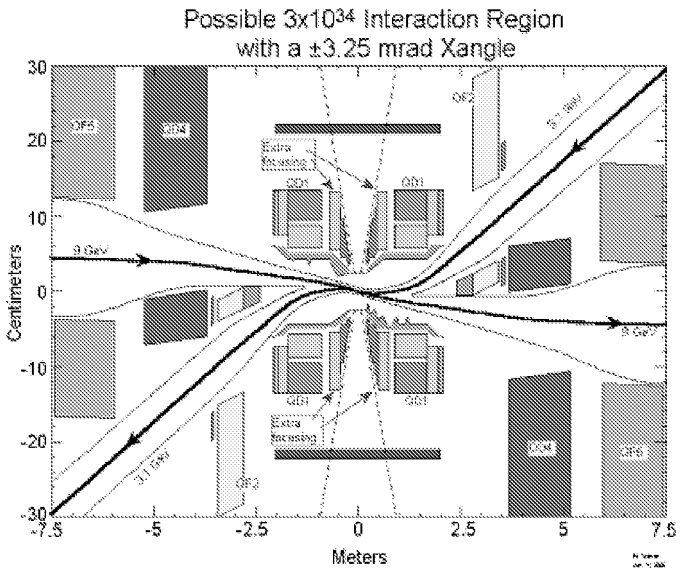

FIG. 26: The IR design of a high luminosity interaction area for PEP-II.

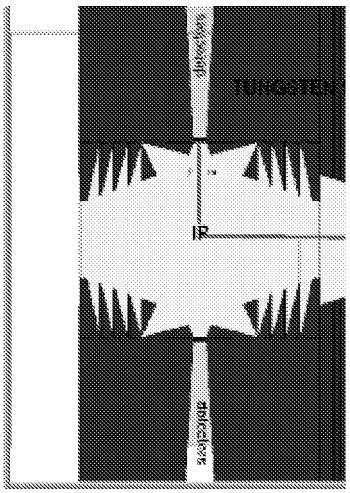

FIG. 27: The IR design for a 4 TeV muon collider.